Magazine of Concrete Research, 2002, **54**, No. 5, October, 321–332

Crack-based analysis of concrete with brittle reinforcement

T. J. Stratford* and C. J. Burgoyne†

FaberMaunsell Ltd; University of Cambridge

Brittle reinforcement (such as fibre-reinforced plastic) is being developed as an alternative to traditional steel reinforcement. The lack of ductility in a brittle-reinforced beam means that there is very little potential for stress redistribution, and the lower-bound theorem of plasticity (which allows many of the assumptions made in steel-reinforced concrete analysis) cannot be applied. Analysis of brittle-reinforced concrete must be based on a detailed examination of compatibility requirements within a beam, of which the cracks form an important part. A crack-based model is developed in this article, based on compatibility requirements where reinforcement crosses a crack, and compatibility in the compression-zone concrete. The analysis incorporates dowel-rupture of the reinforcement, and the reduced strength of a corner of a stirrup. It highlights the need for further research into flexure-shear of the compression zone, dowel-splitting, and local failure of the concrete. The crack-based model is used to illustrate the importance of compatibility in both the flexural and shear analysis of brittle reinforced concrete. In particular, the current proposals for shear design (which assume pseudo-plastic reinforcement) are examined, and contrasted with compatibility requirements within the beam.

Nomenclature

A	cross-sectional area of reinforcement
b	breadth of beam
d	total depth of beam
d_E	effective depth of beam (top-fibre to reinforcement)
e	reinforcement eccentricity (from centre of rectangular beam)
E_F	reinforcement stiffness
E_C	concrete stiffness
F	tensile force in a single piece of reinforcement (including preload)
f_C	compressive strength of concrete
K	bond parameter, describing the compliance of a particular beam section
ℓ_S	length of flexural reinforcement over which there is no transverse restraint, increased by dowel-splitting
M	moment
n	number of pieces of reinforcement
N	axial force
P	preload in a single piece of reinforcement
p	horizontal projected length of crack
q	crack height
s	slip of reinforcement relative to the surrounding concrete, at a crack surface
s_L/s_R	s on the left/right side of a crack
u	increase in unbonded reinforcement length of reinforcement due to local concrete failure
u_L/u_R	u on the left/right side of a crack
V	shear force
w_c	compressive concrete displacement
w_0	displacement at which concrete in compression carries no load
y	position in compression zone: height above crack tip
γ	reduction in the reinforcement strength when pulled at an angle
ε	reinforcement strain (including prestrain)
ε_c	compressive concrete strain
ε_P	reinforcement prestrain
ε_U	reinforcement ultimate axial strain
$\varepsilon_{U\theta}$	reinforcement ultimate strain when pulled at angle θ to its axis

* Maunsell House, 160 Croydon Road, Beckenham, Kent, BR3 4DE, UK.
† University of Cambridge, Engineering Department, Trumpington St., Cambridge, CB2 1PZ, UK.

(MCR 964) Paper received 22 August 2001; last revised 14 November 2001; accepted 19 December 2001

ε_Y	ductile reinforcement yield
η	strain crack opening angle
θ	angle at which reinforcement is pulled relative to its axis
μ	bond parameter, describing magnitude of bond stress
ρ	reinforcement ratio, $\rho = nA/bd_E$
χ	reduction in the shear reinforcement strength at a corner
Ω	bond parameter, describing shape of bond-stress–slip curve

Introduction

Current design techniques for reinforced and prestressed concrete largely avoid considering the cracks within the concrete. For example, flexural design is strain-based and assumes plane sections, implying perfect bond between the concrete and the reinforcement. The truss analogy for shear assumes continuous curvature along a beam, whereas the curvature is localised at the cracks.

By avoiding the details of cracking, the equilibrium state assumed in design does not satisfy compatibility. However, the lower-bound (or safe load) theorem of plasticity states that we can use this equilibrium state safely in design, provided stress redistribution can occur, allowing the required load to be carried.[1]

Stress redistribution requires ductility within the beam. Steel reinforcement is ductile, and hence the details of cracking need not be considered with steel-reinforced concrete. There has been considerable recent research into using fibre-reinforced plastics (FRPs) as concrete reinforcement. These materials are brittle, and thus cannot contribute to stress redistribution.[2] Concrete has limited pseudo-ductility provided it is subjected to triaxial confinement, and limited stress redistribution is possible in a beam subjected to pure flexure. However, under shear loading the concrete is subjected to tensile actions, so that the concrete is brittle.[3] Neither the reinforcement nor the concrete can contribute to stress redistribution in a brittle-reinforced concrete beam.

Since stress redistribution cannot be relied upon in a brittle-reinforced beam, analysis must be based on the actual equilibrium state, which also satisfies compatibility.[1] Analysis must examine compatibility requirements in the region of cracks.

Research into FRP-reinforced concrete (in particular, its shear behaviour) has so far concentrated on adapting the methods of analysis used with (ductile) steel reinforcement. Much important experimental work has been undertaken. However, this has not been accompanied by a fundamental review of the underlying theory to which the experimental results are applied.

This article presents a theoretical investigation. It examines compatibility requirements in the region of a crack, and describes the implications of using brittle reinforcement in concrete.

Crack-based analysis of a single, flexural crack

The simplest crack-based analysis models a single flexural crack, as in Fig. 1. The beam (of total depth d, and effective depth d_E) is split into two rigid blocks by the crack (height q), which rotate relative to each other by an angle η. External actions (axial force, N and moment, M) are applied to the beam.

The magnitude of the external actions (M, N) for a particular crack configuration (q, η) depend on compatibility in the region of the crack. In particular, two components of the beam require consideration

(*a*) compatibility of the compression-zone concrete
(*b*) compatibility of the reinforcement with the concrete to either side of the crack.

Compatibility in the compression zone

The compressive response of concrete is shown schematically in Fig. 2. The ascending branch describes the concrete while it is undamaged, and (like any elastic material) can be characterised by its stress–strain response. However, as the load increases, micro-cracks form within the concrete. The descending branch is dominated by the manner in which these cracks coalesce and grow, and cannot be described in terms simply of the axial strain. The descending branch is not a material property; it depends on triaxial confinement of the concrete to restrain unstable crack propagation.[3]

In a beam, opening of a flexural crack results in compression of the concrete above the crack. Compatibility and equilibrium conditions within the compression zone are complex, since they include localised micro-crack damage and 3D conditions are important to include confinement effects. The rotation capacity of the compression zone is also increased by confinement by shear reinforcement, and depends on the shape of the beam section. Detailed analysis of compatibility within the compression zone is not realistic for design.

The rigid block model (Fig. 1) describes compatibility in a compression-zone of depth ($d_E - q$) by the angle η. A simple constitutive model is required that captures the overall response of the compression zone,

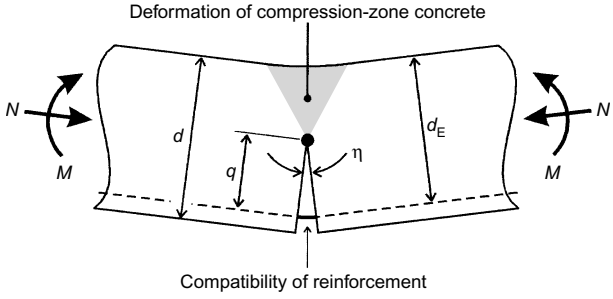

Fig. 1. Rigid block model for a flexural crack

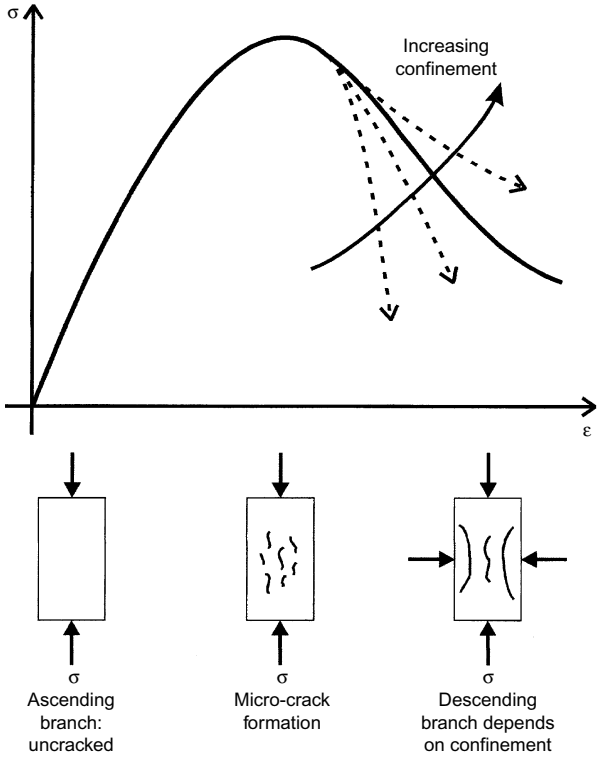

Fig. 2. Concrete in compression

without looking at compatibility in detail. Such a constitutive relationship might be obtained empirically, from a series of beam tests. Alternatively, a detailed finite-element analysis of the compression-zone concrete, capable of correctly modelling confinement effects, might be used to derive a simplified constitutive response. However, these approaches must be the subject of future work.

Simplified compression-zone response. Since accurate constitutive models are not available for the compression-zone concrete, the present work will use a simplified compression-zone model[4] to illustrate crack-based analysis in flexure. This model is based on suggestions by Hillerborg,[5] derived from experimental observations.

At a height y above the crack tip, the displacement of one block relative to the other is $y{\cdot}\eta$ (Fig. 3(a)). Based on tests on under-reinforced beams, Hillerborg proposed using a gauge-length equal to the compression-zone depth $(d_E - q)$ to find the compression-zone strain from the displacement (Fig. 3(b)). A parabolic stress–strain ascending branch is assumed (as shown in Fig. 3(c) for the case $f_C = 34$ MPa, which is used below). Hillerborg also noted that damage of the com-

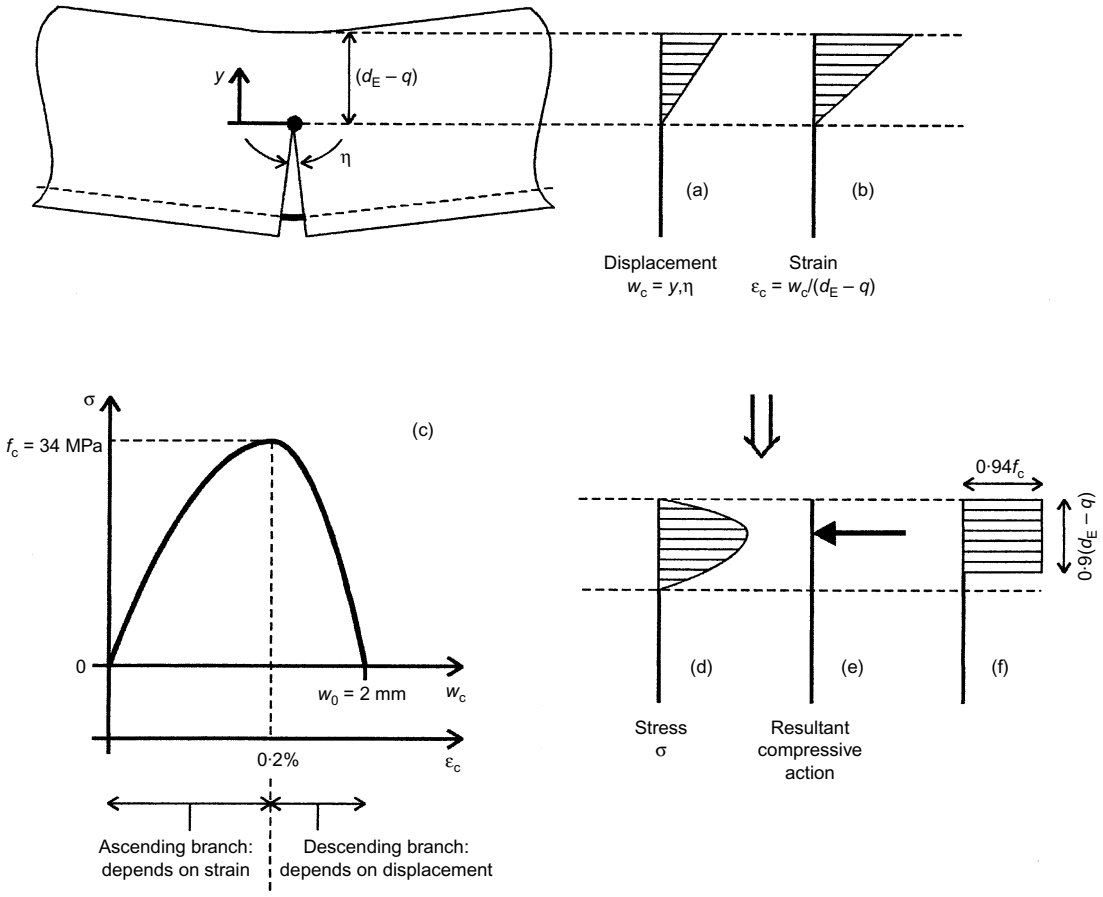

Fig. 3. Idealised constitutive model for compression-zone concrete

pression zone becomes localised at large crack openings. Thus, Hillerborg suggested that the descending branch could be described in terms of displacement (rather than strain). In the present model, a parabolic stress–displacement curve is adopted for the descending branch. As shown in Fig. 3(c), the descending branch is defined by the displacement at which the supported stress returns to zero. A value of $w_0 = 2$ mm is used here, based partly on Hillerborg's work, and partly by comparison with strain-based analyses (as described below).

Integrating the stress distribution given by the ascending and descending branches (Fig. 3(d)) through the compression zone gives the net force, and its position (Fig. 3(e)). A simple constitutive relationship has thus been established between the compression-zone depth ($d_E - q$) and crack opening (η), and the compression-zone force. However, Hillerborg[5] acknowledged that this model requires verification.

Equivalent rectangular stress block for strain-based analysis. Later in this article, an analysis using the displacement-based compression zone model shown in Fig. 3 is compared with the more familiar strain-based approach. Strain-based design simplifies the compression-zone stress distribution to a rectangular stress block, as in Fig. 3(f).

In this article, a constant stress of 0·94 f_C is assumed to act over 90% of the compression-zone depth. This stress block was calibrated using the under-reinforced steel section (described below), so that predictions of the ultimate moment and compression-zone depth at failure agree using crack-based and strain-based analyses.

Note that f_C is the compressive strength of the concrete within the compression zone, where the details of confinement are different from those in a cube or cylinder test.[3] Thus, f_C differs from the concrete strength found in design codes.

Axial compatibility of the flexural reinforcement

The flexural reinforcement must be compatible with the concrete to either side of a crack. As shown in Fig. 4, axial compatibility of the flexural reinforcement is described by the combination of

(*a*) Slip of the reinforcement relative to the surrounding concrete. The slip on the left and right sides of the crack is denoted by s_L and s_R.
(*b*) Stretching of the unbonded reinforcement. The length of reinforcement not bonded to the concrete is the sum of the slip (s_L and s_R), and local concrete failure (u_L and u_R) to either side of the crack. (Local concrete failure is discussed in a subsequent section.)

Compatibility requires that the combination of slip and stretching must equal the separation of the crack surfaces ($q \cdot \eta$):

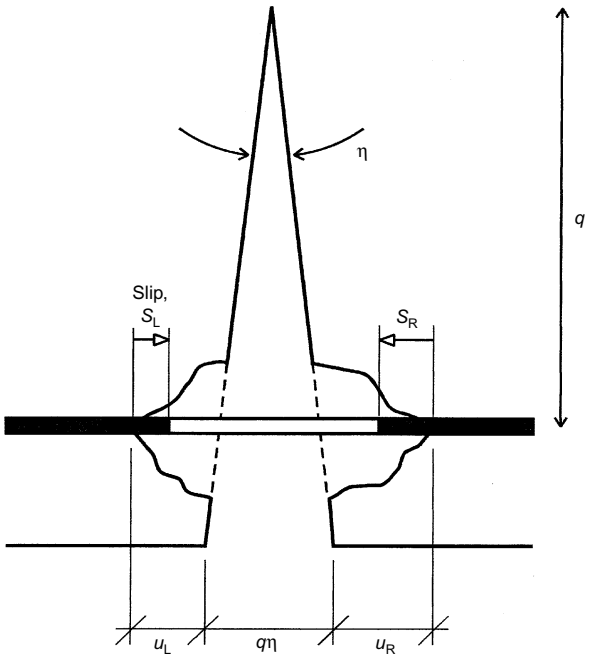

Fig. 4. Compatibility of the flexural reinforcement across a crack

$$\underbrace{(s_L + s_R)}_{\text{Total Slip}} + \underbrace{(s_L + s_R + u_L + u_R)}_{\text{Total unbonded length}} \times \underbrace{(\varepsilon - \varepsilon_P)}_{\text{Reinforcement strain in excess of prestrain}} = \underbrace{q\eta}_{\text{Crack opening}} \quad (1)$$

For the symmetric case, in which the slip and local failure depth to either side of the crack are equal:

$$(1 + \varepsilon - \varepsilon_p)s + (\varepsilon - \varepsilon_p)u = \frac{q\eta}{2} \quad (2)$$

Concrete-reinforcement bond. To apply equation (2), a constitutive relationship is required to describe how the slip (s) increases with axial load (F) and hence strain (ε), in the reinforcement.

Various bond models have been proposed to describe the constitutive response of the concrete-reinforcement interface.[6] Most are derived from tests in which the embedded length is short compared with the bar diameter, whereas the embedded length in a beam is usually long. It might be thought that the short-embedded-length models could be integrated along the length of the reinforcement to give the long-embedded-length response. However, this is only valid if identical bond mechanisms act in both cases. This is unlikely to be the case with FRP reinforcement, due to Poisson ratio effects, and deterioration of the interface at high slips.[7,8]

The pull-out response of reinforcement in a beam must therefore be based on long-embedded-length tests, such as those carried out by Lees[9] with aramid FRP (AFRP) reinforcement. Lees described the pull-out response using a bond-stress–slip curve of the form

$$\tau = \mu s^{\Omega} \tag{3}$$

where μ and Ω describe the form of the interface bond-stress–slip curve and are found empirically.

Once these parameters have been determined, the pull-out of the reinforcement can be described by the following relationship between the reinforcement force (F) and slip (s):[4,9]

$$s = \left\{ \frac{F - P}{AE_F} \sqrt{\frac{1+\Omega}{2\mu K}} \right\}^{2/(1+\Omega)} \tag{4}$$

where K has the dimensions length/force, and describes how the interface bond-stress affects the slip between the concrete and reinforcement, for a specific beam section:[8]

$$K = \frac{2}{E_F}\sqrt{\frac{\pi}{A}}\left[1 + \frac{nA}{bd}\frac{E_F}{E_C}\left\{1 + 12\left(\frac{0{\cdot}5\mathrm{d} - d_E}{d}\right)^2\right\}\right] \tag{5}$$

The parameters describe the breadth of the beam (b), the number (n) of pieces of reinforcement of area A within it, and the stiffness of the concrete (E_C) and reinforcement (E_F).

Substituting for the slip in equation (2) gives an expression that combines compatibility requirements across the crack with the constitutive pull-out response of the reinforcement:

$$(1 + \varepsilon - \varepsilon_P)\left\{ \frac{F - P}{AE_F} \sqrt{\frac{1+\Omega}{2\mu K}} \right\}^{2/(1+\Omega)} + (\varepsilon - \varepsilon_P)u = \frac{q\eta}{2} \tag{6}$$

If the reinforcement is elastic, the reinforcement strain (ε) and prestrain (ε_P) can be found from the reinforcement force (F) and preload (P):

$$\varepsilon = \frac{F}{AE_F} \text{ and } \varepsilon_P = \frac{P}{AE_F} \tag{7}$$

For yielding reinforcement, the reinforcement force (F) remains constant, while the reinforcement strain (ε) continues to increase.

Equation (6) can be solved numerically to find the reinforcement strain (ε) and the reinforcement force (F) from the crack width ($q\eta$).

Reinforcement failure. Failure of the reinforcement depends on the reinforcement strain (ε). For brittle reinforcement, failure occurs when the ultimate strain (ε_U) is reached.

Ductile reinforcement is elastic until the yield strain (ε_Y) is reached. For larger crack widths, the reinforcement force remains constant ($F = AE_F\varepsilon_Y$), while the strain continues to increase. Failure occurs at the strain capacity (ε_U) of the reinforcement.

Local concrete failure. Local concrete failure describes a localised failure of the surface concrete around the reinforcement, which can occur as the reinforcement is pulled out of the concrete (Fig. 4). The depth of the failure can be large compared with the crack width. Local failure has been observed by Kanematsu *et al.*[10] with FRP reinforcement, and was included in equation (2).

Local failure occurs if the force transferred across the reinforcement–concrete interface (which depends on its bond characteristics) exceeds the strength of a conical surface within the concrete. Goto *et al.*[11] considered a similar conical concrete failure for steel anchor bolts, and their analysis can be adapted for reinforcement pull-out.[4]

Ideally, the local failure depth (u) could be found for a given reinforcement force (F). However, it is not possible to find a single value of the failure depth without knowing the size of initial imperfection. The initial imperfection describes the roughness of the crack surface, and thus depends on the local arrangement of aggregate in the vicinity of the reinforcement, which is random. Since the initial imperfection cannot be predicted, a specific value of u cannot be determined. (A detailed analysis can be found in Stratford.[4])

For the purposes of this article, a single representative failure depth will be used for all values of F. The analysis could be refined by assuming that u varies as some function of F.

Examples using the flexural single crack model

The models described above for the compression-zone concrete and compatibility of the reinforcement across a crack can be combined to predict the flexural response of a beam.[4]

Crack-based analysis with ductile reinforcement. Before applying the crack-based analysis to brittle reinforcement, it is sensible to verify the technique with familiar, steel reinforcement. This example considers the rectangular beam section shown in Fig. 5, with the concrete model of Fig. 3.

Table 1 lists the different reinforcement arrangements, and the associated material and bond properties (as given by Lees[9]). Three steel-reinforced concrete sections are considered.

(*a*) Ordinary, under-reinforced concrete, with high-yield steel ($\rho = 0{\cdot}039$).
(*b*) Ordinary, over-reinforced concrete, with high-yield steel ($\rho = 0{\cdot}049$).
(*c*) Prestressed concrete, prestressed to 60% of tendon yield.

The reinforcement ratio ($\rho = nA/bd_E$) was chosen using strain-based design methods. A balanced section (in which reinforcement yield and failure of the compression-zone concrete occur simultaneously) requires $\rho = 0{\cdot}046$. The under-reinforced section has a smaller

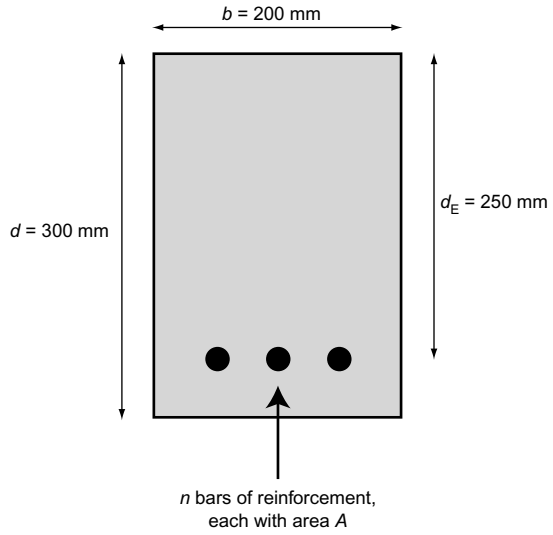

Fig. 5. Dimensions of beam section considered in the examples

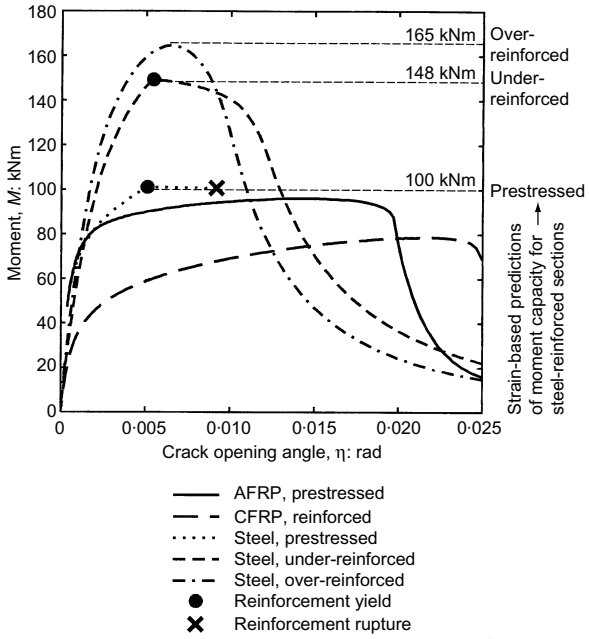

Fig. 6. Moment–deflection responses predicted by the single flexural crack model

reinforcement ratio, and hence fails by reinforcement yield, while the over-reinforced section fails in the compression zone (usually avoided with steel reinforcement, since failure is brittle).

The crack-based analysis (Fig. 6) confirms the failure modes predicted by the strain-based analysis. For the under-reinforced section, the steel yields before the full capacity of the compression zone can be exploited. As the crack opening angle increases, reinforcement yield is accompanied by degradation of the compression-zone concrete, so that the moment supported by the section drops to zero. For the over-reinforced section, the reinforcement does not yield, and the response is characterised solely by failure of the compression-zone concrete. Fig. 6 also shows the response of a steel-prestressed concrete section, which is dominated by yield of the tendons. Due to the prestress and the smaller strain capacity of prestressing steel (compared with high-yield steel), failure occurs when the strain capacity of the reinforcement is reached. The ultimate moments predicted by the crack-based analysis agree with those found using strain-based design (shown to the right of the figure). As described above, the under-reinforced steel section was used to calibrate the rectangular stress block used for strain-based design.

Crack-based analysis with brittle reinforcement. With steel reinforcement, strain-based analysis is adequate for design (since lower-bound plasticity theory

Table 1. Reinforcement properties for crack-based flexural analysis example

Property	Units	High-yield steel		Pre-stressing steel	CFRP	AFRP (Technora)
		Under-reinforced	Over-reinforced			
Number of bars/tendons (n)	–	4	5	3	2	3
Bar diameter	mm	25·0		10·8	16·0	10·0
Prestress as proportion of tendon strength	%	0		60	0	60
Bond parameter (Ω)	–	0·4			−0·5	
Bond parameter (μ)	MPa mm$^{-\Omega}$	13·5			5·7	
Yield strength ($E_F \cdot \varepsilon_Y$)	MPa	400		1700	–	
Ultimate strain (ε_U)	%	10·0		4·0	1·0	3·7
Stiffness (E_F)	GPa	200		220	100	54·0
Local failure depth (u)	mm	10				

can be applied with ductile reinforcement). With brittle reinforcement, compatibility must be examined in detail, and a crack-based analysis is more relevant. Fig. 6 includes the moment–deflection response of two brittle-reinforced sections.

(*a*) Ordinary reinforced concrete, with CFRP reinforcement ($\rho = 0{\cdot}0080$).
(*b*) Prestressed concrete, with AFRP tendons ($\rho = 0{\cdot}0047$).

Details are again given in Table 1. (Note that the net strength of the AFRP tendons is the same as the prestressed steel tendons.)

The quantity of steel reinforcement is usually chosen to avoid failure in the compression zone. With brittle reinforcement, however, compression-zone failure is desirable, since it is more ductile than reinforcement rupture. Strain-based analysis suggests that compression-zone failure can be ensured if the reinforcement ratio exceeds the brittle reinforcement ratio (equivalent to the balanced section ratio with ductile reinforcement).[12]

For the AFRP-prestressed section used in Fig. 6 the reinforcement ratio is far greater than the brittle reinforcement ratio ($\rho = 0{\cdot}0017$), and should therefore guarantee failure in the compression-zone concrete. Similarly, for the CFRP-reinforced section, the reinforcement ratio is greater than the brittle reinforcement ratio ($\rho = 0{\cdot}0075$).

For both the CFRP-reinforced and AFRP-prestressed sections, the crack-based analysis does indeed predict failure in the compression-zone concrete.

Variation of reinforcement-concrete bond. Nanni *et al.*[7] noted that the load carried by flexural reinforcement depends on the bond characteristics of the concrete–reinforcement interface. This can be studied using the crack-based model.

Figure 7 shows the moment–deflection response of various AFRP-prestressed sections. The beam section and the reinforcement ratio are the same as those used above. However, the number of tendons (n) is varied, since the surface area available for concrete–reinforcement bond increases with the number of tendons.

Increasing the concrete–reinforcement bond increases the moment capacity of the section. However, compatibility of the reinforcement across the crack (equation (2)) means that the reinforcement strain increases with the bond. Consequently, the failure mode changes from compression-zone failure (for $n = 2$, 3) to tendon rupture (for $n = 4$, 5, 6).

It is widely believed that high bond strength must be available to make effective use of the strength of FRP reinforcement. However, low bond strength can support a high load over a longer length of the concrete–reinforcement interface.[2] Indeed, this example shows that a high bond strength is undesirable, since it promotes brittle rupture of the reinforcement.

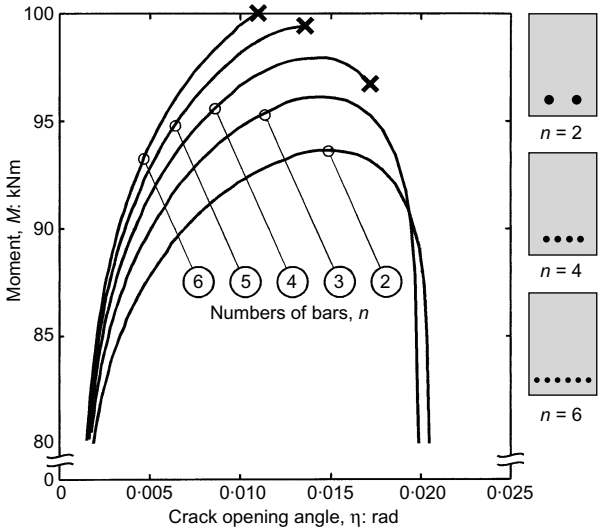

Fig. 7. Moment–deflection response of AFRP-reinforced sections with the same reinforcement ratio, but different numbers of tendons

All the beams have the same reinforcement ratio, which is greater than the brittle reinforcement ratio. Thus, strain-based design predicts that tendon rupture should not occur. However, the strain-based analysis only gives the amount of reinforcement required for failure to start in the compression zone. It is still possible for the reinforcement to rupture before the full rotation capacity of the compression zone has been exploited. With brittle reinforcement, compatibility of the reinforcement with the concrete must be considered.

Crack-based analysis of a single, straight, shear crack

Crack-based analysis is not limited to flexural cracks; it can also be applied to shear cracks. Indeed, shear failure is often brittle and requires particular attention to be paid to compatibility. For example, with steel reinforcement, the quality of the reinforcement–concrete bond is a governing factor in shear failure.[13,14]

Crack-based models for shear are not new: a number have been proposed to describe shear-compression failure.[15] However, these shear-compression models were developed for steel-reinforced concrete, and they do not consider bond and local failure effects in detail. (Models for shear-compression in steel-reinforced concrete can rely on stress redistribution.) Furthermore, most are limited to beams without shear reinforcement.

In this section, a single, straight shear crack (Fig. 8) will be used to illustrate the importance of compatibility in shear analysis with brittle reinforcement. In addition to the nomenclature already introduced, the horizontal projected length of the crack is p, and an external shear load of V is applied to the beam.

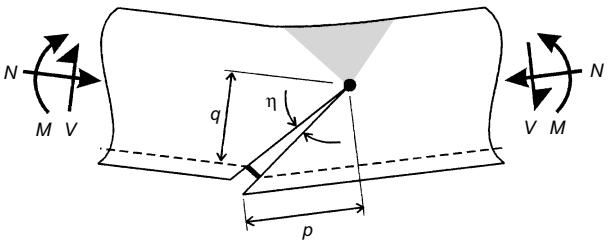

Fig. 8. Single, straight shear crack model

Compatibility in the compression zone

In the flexural case, it is possible to adopt an idealised constitutive model for the compression-zone concrete (such as that suggested above). The addition of shear action considerably increases the complexity of the stress state, and there is no obvious simple constitutive model.

The 'state-of-the-art' for predicting the *capacity* of compression-zone concrete subjected to flexure-shear is Kani's 'shear valley', derived from tests on beams without shear reinforcement.[3,13] The original (1964) 'shear valley' concept has been refined by many researchers, but remains empirical.[4] It is based on tests using steel-reinforced concrete, and thus cannot be directly applied to FRP-reinforced concrete. Furthermore, the shear valley only predicts failure, and does not describe compatibility, which must be considered when brittle shear reinforcement is introduced into a beam.

Further work is required to determine a constitutive relationship for compression-zone concrete subjected to both flexural and shear actions.

Shear compatibility of the flexural reinforcement

Axial compatibility of the flexural reinforcement (as described above) is also important in shear, since the quality of the concrete–reinforcement bond is a governing factor in shear failure.[13,14] However, where the flexural reinforcement crosses the base of an inclined crack, it is also subjected to shear deformation (see Fig. 8). This shearing is described as dowel action.

Kotsovos and Pavlović[3] have suggested that the load carried by dowel action in steel-reinforced beams is negligible compared with that carried by the compression-zone concrete. With FRP reinforcement (which has a low transverse stiffness) an even smaller load will be carried by dowel action.[10]

The load carried may be negligible, but dowel action leads to two important modes of failure

(*a*) dowel-splitting of the concrete along the reinforcement
(*b*) dowel-rupture of the reinforcement.

Dowel-splitting of the concrete. Dowel action by the reinforcement is reacted by tensile stress in the concrete. Dowel-splitting occurs if the tensile strength of the concrete is reached, and describes failure of the concrete along the line of the flexural reinforcement (Fig. 9(a)).

Wedging action when a deformed bar is pulled out of concrete (or when prestress is transferred to the concrete) results in similar tensile stresses in the concrete.[7] To predict dowel-splitting, therefore, the tensile stress due to both dowel action and axial pull-out of the reinforcement must be considered. There has not yet been a detailed investigation of this interaction, although work has been undertaken by Sakai *et al.*[16]

Dowel-splitting can be controlled by including shear reinforcement in a beam (Fig. 9(b)). The stirrups enclose the flexural reinforcement and hence support it, reducing the tensile stress in the concrete.[17] Dowel-splitting increases the length of unbonded flexural reinforcement at the base of a crack. Consequently, a larger crack width is required for the flexural reinforcement to support the same load (F). Rapid crack propagation follows dowel-splitting, a typical mode of failure in beams with long shear-spans.[3]

Dowel-rupture of the reinforcement. Dowel-rupture describes the reduction in axial load capacity of a piece of reinforcement when it is also subjected to shear (as at the base of the crack in Fig. 9). Chana[17] noted this effect with steel reinforcement, although in that case it does not dominate failure. FRP reinforcement is brittle and has low transverse strength, so

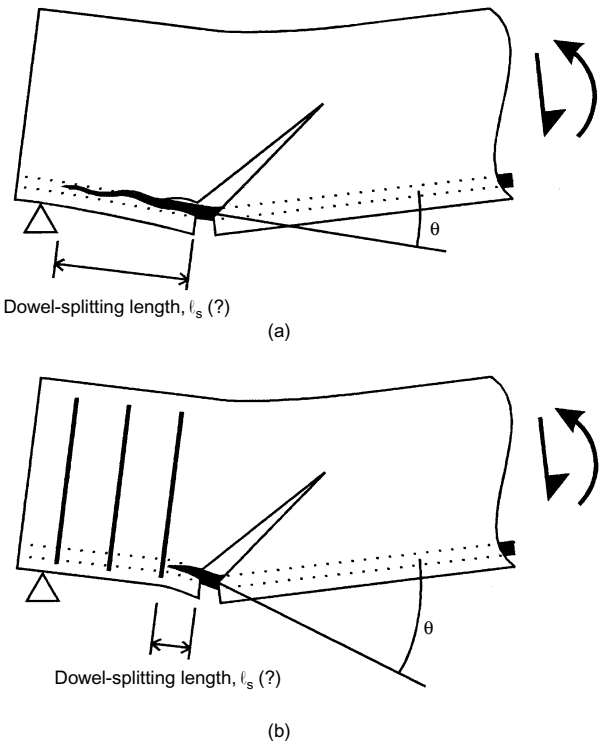

Fig. 9. Dowel-splitting of the concrete and the angle (θ) governing dowel-rupture of the flexural reinforcement: (a) with; (b) without shear reinforcement

dowel-rupture can be a dominant mode of shear failure.[18,19] Maruyama *et al.*[20] (for example) investigated dowel-rupture of FRP reinforcement, and suggested an expression for the capacity of reinforcement pulled at an angle θ to its axis. Maruyama's expression is in terms of the reinforcement stress, but can be written in terms of strain:

$$\varepsilon_{U\theta} = \varepsilon_U(1 - \gamma\theta) \tag{8}$$

where ε_U is the axial strain capacity of the reinforcement, $\varepsilon_U\theta$ is the strain capacity of the reinforcement pulled at an angle θ (in radians) to its axis, and γ is the strength reduction factor, which depends on the reinforcement and must be determined empirically.

The angle θ is the reinforcement direction relative to the direction of crack opening. θ depends on the crack opening perpendicular to the reinforcement direction ($p.\eta$), and the length of reinforcement over which there is no transverse restraint (ℓ_S), which is increased by dowel-splitting (Fig. 9):

$$\tan\theta = \frac{p\eta}{\ell_S} \tag{9}$$

The dowel-splitting length. Enclosing the flexural reinforcement in stirrups prevents dowel-splitting of the concrete, but it also increases θ and hence promotes dowel-rupture of the reinforcement. The dowel-splitting length (ℓ_S) is an important parameter in predicting the shear capacity of concrete beams with brittle reinforcement.

Further work is required before the dowel-splitting length can be predicted. In a beam without shear reinforcement, the dowel-splitting length might be assumed to extend to the support position (Fig. 9(a)). For a beam with shear reinforcement, the dowel-splitting length might be taken as the stirrup spacing (Fig. 9(b)), although the actual length will depend upon the position of the stirrup nearest to the base of the crack. However, these assumptions are not necessarily safe, since stress redistribution is not possible when brittle materials are used.

Compatibility of the shear reinforcement

Shear reinforcement carries tensile actions across inclined cracks as they propagate into a beam. Like flexural reinforcement, shear reinforcement must be compatible with the local crack opening. A long-embedded-length bond model is required to describe pull-out of the reinforcement, and this must be combined with stretching of the unbonded reinforcement, including local failure of the concrete.[4]

Mechanical interlock occurs at a bend in shear reinforcement. Ideally, the pull-out model would consider the transfer of load from reinforcement to concrete around the bend. Furthermore, the shear reinforcement is often weakened at a bend, depending upon the technique used to form the corner, and its radius. Corner strengths lower than 50% of the strength of the straight reinforcement have been reported.[21] There have been attempts to model the strength of the corner using finite element techniques, but at the present time it is sensible to base design on empirical values for the reinforcement being used. To determine whether failure occurs at a bend in the shear reinforcement, the force in the shear reinforcement at that point must be found by considering the load transferred across the concrete–reinforcement interface.

Alternatively, dowel-rupture of the shear reinforcement may occur at the crack surface, as for flexural reinforcement.

An example using the single shear crack model

Figure 10 shows a crack in the shear-span of a beam, angled at 40° to the beam axis. The CFRP-reinforced beam section from the flexural example is used. Three CFRP stirrups cross the crack, the details of which are given in Table 2. Further research is needed to provide accurate models for dowel-splitting and the flexure-shear response of compression-zone concrete. In the present example, the unbonded length of reinforcement (u) to either side of the crack is increased to 40 mm (half the stirrup spacing), and the descending branch response of the concrete is shortened by taking $w_0 = 1$ mm (Fig. 3). Whilst accurate quantitative predictions are not possible, the single shear crack analysis can be used to qualitatively illustrate the importance of compatibility in a beam with brittle reinforcement.

Figure 11 gives the moment–deflection responses predicted by the crack-based analysis. The moment has been normalised by the moment capacity of the beam without shear reinforcement.

The action of brittle shear reinforcement. The responses of beams with brittle shear reinforcement, and without shear reinforcement are plotted in Fig. 11. As expected, adding shear reinforcement increases the shear capacity of the beam. Failure is brittle, by rupture of the stirrup nearest the base of the crack, where the crack width is greatest. (In this case, dowel-rupture of the stirrup occurs, rather than failure at a corner of the stirrup.) Failure of the second stirrup from the base of the crack follows next, giving a second (lower) peak in the moment–deflec-

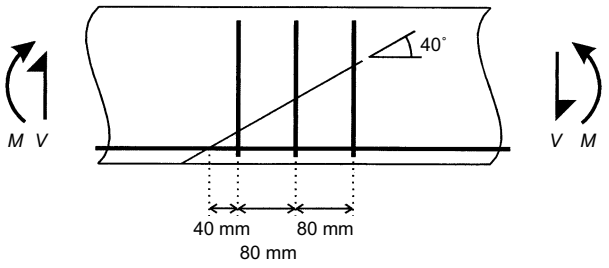

Fig. 10. Geometry of the single shear crack example, showing the shear reinforcement arrangement

Table 2. Reinforcement properties for crack-based shear analysis example

	Property	Units	Value
CFRP flexural reinforcement and concrete	Local failure depth (flexural reinforcement) (u)	mm	40
	End of concrete descending branch in compression (w_0)	mm	1
	Reduction in reinforcement strength when pulled at an angle (γ)	–	1·2
	Other values as for the flexural example		
CFRP shear reinforcement	Stirrup diameter	mm	8·0
	Strength reduction factor at a corner of a stirrup (χ)	–	0·8
	Local failure depth (shear reinforcement)	mm	10
	Stiffness, bond parameters and strength when pulled at an angle of the shear reinforcement as for CFRP flexural reinforcement		

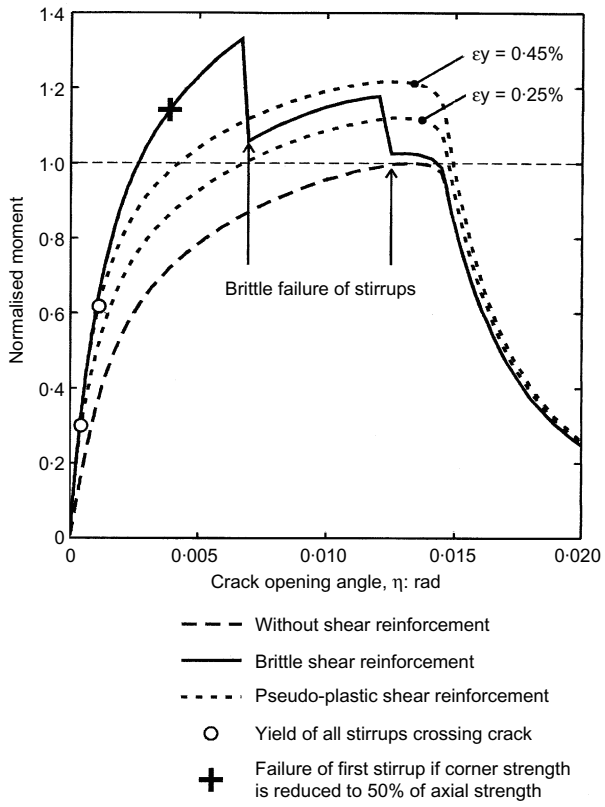

Fig. 11. Moment–deflection responses predicted by the single shear crack model

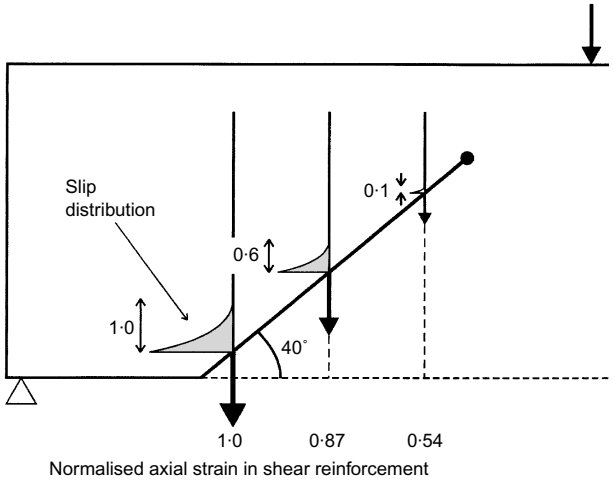

Fig. 12. The variation in shear reinforcement strain and concrete-reinforcement slip along a shear crack, just before failure of the first stirrup.

tion curve. The third stirrup carries very little load, since it is close to the crack tip (Fig. 10), and hence the remaining response is similar to that for a beam without shear reinforcement.

Figure 12 shows the axial strain in the shear reinforcement just before failure of the first stirrup (normalised by the strain in the first stirrup). The relative lengths of the concrete–reinforcement slip distributions are also indicated in the figure. The stirrup strain varies along the crack (as shown experimentally by Zhao *et al.*[22]). The distribution of strain along the crack depends on the crack geometry, the position of the stirrups relative to the base of the crack, the depth of local concrete failure and the bond characteristics of the concrete–reinforcement interface. Thus, if two beams have shear reinforcement with the same ultimate strain capacity but different bond characteristics, the net load carried by the stirrups will differ.

The 'concrete contribution'. The shear capacity of a concrete beam is commonly separated into the components carried by the concrete and by the stirrups. For steel-reinforced concrete, the 'concrete contribution' is taken as the shear capacity of an equivalent beam without shear reinforcement.

The current shear design proposals for FRP-reinforced concrete (described in Guadagnini *et al.*[23]) take the 'concrete contribution' of a steel-reinforced concrete beam, and modify it by the reduced stiffness of the FRP reinforcement. This 'concrete contribution' has been validated by tests on beams without shear reinforcement. However, Fig. 11 shows that in a beam

with stirrups, the load carried by the concrete at failure is determined by compatibility of the cracked concrete with the shear reinforcement. This is not reflected by the code proposals. Fig. 11 shows that the crack opening angle at failure of the beam with brittle stirrups ($\eta \approx 0{\cdot}007$) is less than for a beam without shear reinforcement ($\eta \approx 0{\cdot}013$). Thus, the compression-zone concrete in the beam with shear reinforcement supports only 85% of the shear capacity of a beam without shear reinforcement.

The 'stirrup contribution'. The current design code proposals for FRP-reinforced concrete use truss analogies to assess the 'stirrup contribution'.[23] Truss analogies assume that all stirrups along the shear-span of a beam carry the same stress.[3] For steel reinforcement, this is the yield stress.

FRP reinforcement does not yield, and the stirrup strain varies both generally along the shear-span (Fig. 12), and also due to the nearby crack geometry. The code proposals assume an artificial stirrup yield strain (the 'allowable strain') for use in the truss analogy. Thus, for shear design, the brittle FRP reinforcement is modelled by an imaginary pseudo-plastic FRP reinforcement.

The crack-based analysis can be used to examine the effect of assuming pseudo-plastic FRP reinforcement. Fig. 11 includes two such analyses, for stirrup 'yield strains' of $\varepsilon_Y = 0{\cdot}25\%$ (suggested by the *Eurocrete* project[24]), and $\varepsilon_Y = 0{\cdot}45\%$ (proposed in 'The Sheffield approach[23]).

The shear capacity predicted using pseudo-plastic FRP reinforcement is lower than with brittle reinforcement. However, the pseudo-plastic FRP reinforcement analysis is not necessarily conservative. For example, the brittle reinforcement analysis assumes that the corner strength of a stirrup is $\chi = 80\%$ of its straight strength. If this is reduced to $\chi = 50\%$,[21] the brittle-reinforced beam fails at a normalised moment of 1·15 ('+' in Fig. 11), which is lower than the pseudo-plastic FRP prediction.

The pseudo-plastic FRP analysis does not predict the individual stirrup failure events. Furthermore, the crack-opening angle at failure of a psuedo-plastic FRP reinforced beam is much greater than that with brittle reinforcement.

The original intention of the 'allowable strain' concept[24] was to limit the stirrup strain so that the crack width at failure was similar to that in steel-reinforced concrete, thus allowing the full 'concrete contribution' to be developed. However, the crack-based analysis shows that the 'yield strain' of the stirrups is reached at a crack opening angle of $\eta \approx 0{\cdot}001$ ('O' in Fig. 11), whereas the shear capacity of a beam without shear reinforcement requires $\eta \approx 0{\cdot}013$. The 'allowable strain' concept does not consider compatibility of the shear reinforcement with the cracked concrete, which the crack-based analysis shows is necessary for shear design.

Conclusions

With steel reinforcement, we are used to making assumptions about the equilibrium state in a concrete beam, such as the assumption that the 'stirrup' and 'concrete' contributions can be superimposed in shear analysis. If we are to use brittle reinforcement, such assumptions are not safe. Stress redistribution cannot be relied upon within the beam, and compatibility requirements must be considered. The importance of compatibility is illustrated by dowel-rupture of the flexural reinforcement, and the variation in stirrup strain along a crack. Both of these are crucial in predicting the shear capacity of a brittle-reinforced beam. The current shear design proposals for FRP-reinforced concrete do not consider compatibility.

This article does not pretend to provide all the answers to shear analysis of brittle-reinforced concrete. However, crack-based modelling offers a more valid approach to analysis, since it considers compatibility requirements in detail. The models developed in this article have allowed the importance of concrete–reinforcement bond and action of the shear reinforcement to be examined.

This article has only considered a single, straight crack, at a known position in the beam. In reality, there are multiple, curved cracks, requiring a more complex model for compatibility within the beam, and an assessment of the paths of crack propagation.[4]

Research on FRP-reinforced concrete has largely focused on the properties of the reinforcement, for example: dowel-rupture of reinforcement, pull-out bond tests, or failure of shear reinforcement at a bend. Understanding the reinforcement is vital, but it must be accompanied by research into the concrete. The concrete models used for steel-reinforced concrete are not sufficiently detailed for use with brittle reinforcement (where stress redistribution cannot be relied upon). In particular, compatibility in the compression-zone concrete is not described; the model used here requires verification for flexural analysis, and is inadequate for shear analysis. Dowel-splitting of the concrete, and local failure of the concrete around the reinforcement are also important if brittle reinforcement is used.

Experimental studies are planned to confirm the results presented in this article. The work will result in a better understanding of compatibility conditions throughout a beam, which is necessary to describe shear in a concrete beam with brittle reinforcement.

References

1. STRATFORD T. J. and BURGOYNE C. J. Shear analysis of concrete with brittle reinforcement. *Proc. 5th International Symposium on Non-metallic (FRP) Reinforcement for Concrete Structures*, Cambridge 2001, 939–948.
2. BURGOYNE C. J. Rational use of advanced composites in concrete. *Proc. 3rd International Symposium on Non-metallic (FRP)*

Reinforcement for Concrete Structures, Japan Concrete Institute, Tokyo, 1997, Vol.1, 75–88.
3. KOTSOVOS M. D. and PAVLOVIĆ M. N. *Ultimate limit-state design of concrete structures – A new approach*. Thomas Telford Ltd, London, 1999.
4. STRATFORD T. J. The shear of concrete with elastic FRP reinforcement. PhD thesis, Department of Engineering, University of Cambridge, UK, 2000.
5. HILLERBORG A. Size dependency of the stress-strain curve in compression. *Proc. International Rilem workshop 6*, Analysis of concrete structures by fracture mechanics, 1991, 171–178.
6. COSENZA E., MANFREDI G. and REALFONZO R. Behavior and modelling of bond of FRP rebars to concrete. *ASCE Journal of Composites for Construction*, 1997, 1, No. 2, 40–51.
7. NANNI A., BAKIS C. E. and BOOTHBY T. E. Test methods for FRP-concrete systems subjected to mechanical loads: State of the art review. *Journal of Reinforced Plastics and Composites* 1995, 14, No. 6, 524–558.
8. STRATFORD T. J. and BURGOYNE C. J. Bond models for analysing beams with brittle FRP reinforcement. In preparation.
9. LEES J. M. Flexure of concrete beams pre-tensioned with aramid FRPs. PhD thesis, Department of Engineering, University of Cambridge, UK, 1997.
10. KANEMATSU H., SATO Y., UEDA T. and KAKUTA Y. A study on failure criteria of FRP rods subject to tensile and shear force. *Proc. FIP '93 Symposium – Modern prestressing techniques and their applications*, Japan Prestressed Concrete Engineering Association, Tokyo, 1993, Vol. 2, 743–750.
11. GOTO Y., OBATA M., MAENO H. and KOBAYASHI Y. Failure mechanism of new bond-type anchor bolt subject to tension. *ASCE Journal of Structural Engineering* 1993, 119, No. 4, 1168–1187.
12. DOLAN C. W. and BURKE C. R. Flexural strength design of FRP prestressed beams. *Proc. Advanced Composite Materials in Bridges and Structures – 2nd International Conference*, The Canadian Society for Civil Engineering, 1996, 383–390.
13. KANI G. N. J. The riddle of shear failure and its solution. *Journal of the ACI*, 1964, 61, No. 4, 441–467.
14. BAŽANT Z. P. and KAZEMI M. T. Size effect on diagonal shear failure of beams without stirrups. *ACI Structural Journal*, 1991, 88, No. 3, 268–276.
15. REGAN P. E. Research on shear: a benefit to humanity or a waste of time? *The Structural Engineer*, 1993, 71, No. 19, 337–347.
16. SAKAI T., KANAKUBO K., YONEMARU K. and FUKUYAMA H. Bond splitting behavior of continuous fiber reinforced concrete members. *Proc. 4th International Symposium on Fibre Reinforced Polymer Reinforcement for Reinforced Concrete Structures*, SP-188, ACI, Michigan, 1999, 1131–1144.
17. CHANA P. S. Analytical and experimental studies of shear failures in reinforced concrete beams *Proc. Instn Civ. Engrs Part 2*, 1988, 85, 609–628.
18. BANK L. C. and OZEL M. Shear failure of concrete beams reinforced with 3-D fiber reinforced plastic grids. *Proc. 4th International Symposium on Fibre Reinforced Polymer Reinforcement for Reinforced Concrete Structures (SP-188)*, ACI, Michigan, 1999, 145–156.
19. NAAMAN A. E. and PARK S. Y. Shear behavior of concrete beams prestressed with CFRP tendons: preliminary tests evaluation. *Proc. 3rd International Symposium on Non-metallic (FRP) Reinforcement for Concrete Structures*. Japan Concrete Institute, Tokyo, 1997, Vol. 2, 679–686.
20. MARUYAMA K., HONMA M. and OKAMURA H. Experimental study on the diagonal tensile characteristics of various fibre reinforced plastic rods. *Transactions of the Japan Concrete Institute*, 1989, 11, 193–198.
21. MACHIDA A. (ed.) *State of the Art Report on continuous fiber reinforcing materials*. Concrete Engineering Series 3, Research Committee on Continuous Fiber Reinforcing Materials, Japanese Society of Civil Engineers, 1993.
22. ZHAO W., MARUYAMA K. and SUZUKI H. Shear behaviour of concrete beams reinforced by FRP rods as longitudinal and shear reinforcement. *Proc. Non-metallic (FRP) Reinforcement for Concrete Structures (FRPRCS-2)*, E&FN Spon, London, 1995, 352–359.
23. GUADAGNINI M., PILAKOUTAS K. and WALDRON P. Shear design for fibre reinforced polymer reinforced concrete elements. *Proc. 4th International Symposium On Fibre Reinforced Polymer Reinforcement for Reinforced Concrete Structures, Selected Presentation Proceedings*, ACI, Michigan, 1999, 11–21.
24. CLARKE J. L. and O'REGAN D. P. Design of concrete structures reinforced with fibre composite rods. *Proc. Non-metallic (FRP) Reinforcement for Concrete Structures (FRPRCS-2)*, E&FN Spon, London, 1995, 646–653.

Discussion contributions on this paper should reach the editor by 1 April 2003